Crystal responses to general dark matter-electron interactions

Journal of Physics: Conference Series **2156** (2022) 012027 doi:10.1088/1742-6596/2156/1/012027

Crystal responses to general dark matter-electron interactions

Einar Urdshals

Chalmers University of Technology, Department of Physics, SE-412 96 Göteborg, Sweden

E-mail: urdshals@chalmers.se

Abstract. In [1] we develop a non-relativistic effective field theory (NR-EFT) based framework with which rates of dark matter (DM) induced electron hole pair creation in silicon and germanium crystals can be obtained for any form of non-relativistic DM-electron interactions with spin 1/2 DM. We find that the crystal physics is captured by 5 crystal response functions, 4 of which are novel to that work, and we evaluate them using a state of the art DFT calculation.

1. Introduction

With the growing attention directed towards dark matter (DM) electron scattering in the quest for detecting DM with masses below the well explored GeV range down to below an MeV, it is crucial to have a theoretical understanding of DM electron interactions. Previously one has largely focused on the simplest scenarios of DM electron interactions, such as the dark photon model. Using non-relativistic effective field theory (NR-EFT) we derive the rate of DM induced electron hole excitations in silicon and germanium crystals.

2. DM and crystal responses

We expand the DM electron interaction matrix element in non-relativistic operators,

$$\mathcal{M}(\mathbf{q}, \mathbf{v}_{\text{el}}^{\perp}) = \sum_i \left(c_i^s + c_i^\ell \frac{q_{\text{ref}}^2}{|\mathbf{q}|^2} \right) \langle \mathcal{O}_i \rangle \,, \tag{1}$$

where the operators $\mathcal{O}_i$ are given in table 1 and their contributions to the rate are given in figure 1, $q_{\text{ref}} = \alpha m_e$ is the reference momentum, and c_i^s (c_i^ℓ) denotes the short (long) range coupling of operator $\mathcal{O}_i$. We find that the rate of electron hole pair creation can be written as [1]

$$\mathscr{R}_{\text{crystal}} = \frac{n_\chi N_{\text{cell}}}{128\pi m_\chi^2 m_e^2} \int \mathrm{d}(\ln \Delta E) \int \mathrm{d}q\, q\, \widehat{\eta}\,(q, \Delta E) \sum_{l=1}^{5} \Re \left(R_l^*(q, v) \overline{W}_l(q, \Delta E) \right) \,, \tag{2}$$

where

$$\begin{aligned} \overline{W}_l(q, \Delta E) =& (4\pi)^2 V_{\text{cell}} \frac{\Delta E}{q^2} \sum_{\Delta \mathbf{G} i i'} \int_{\text{BZ}} \frac{\mathrm{d}^3 k}{(2\pi)^3} \int_{\text{BZ}} \frac{\mathrm{d}^3 k'}{(2\pi)^3}\, B_l \\ & \times \delta(\left|\mathbf{k} - \Delta\mathbf{G} - \mathbf{k}'\right| - q) \delta(\Delta E - E_{i\mathbf{k}} + E_{i'\mathbf{k}'}) \,. \end{aligned} \tag{3}$$

$\mathcal{O}_1 = \mathbb{1}_{\chi e}$	$\mathcal{O}_7 = \mathbf{S}_e \cdot \mathbf{v}_{\rm el}^{\perp}$	$\mathcal{O}_{12} = \mathbf{S}_\chi \cdot \left(\mathbf{S}_e \times \mathbf{v}_{\rm el}^{\perp}\right)$
$\mathcal{O}_3 = i\mathbf{S}_e \cdot \left(\frac{\mathbf{q}}{m_e} \times \mathbf{v}_{\rm el}^{\perp}\right)$	$\mathcal{O}_8 = \mathbf{S}_\chi \cdot \mathbf{v}_{\rm el}^{\perp}$	$\mathcal{O}_{13} = i\left(\mathbf{S}_\chi \cdot \mathbf{v}_{\rm el}^{\perp}\right)\left(\mathbf{S}_e \cdot \frac{\mathbf{q}}{m_e}\right)$
$\mathcal{O}_4 = \mathbf{S}_\chi \cdot \mathbf{S}_e$	$\mathcal{O}_9 = i\mathbf{S}_\chi \cdot \left(\mathbf{S}_e \times \frac{\mathbf{q}}{m_e}\right)$	$\mathcal{O}_{14} = i\left(\mathbf{S}_\chi \cdot \frac{\mathbf{q}}{m_e}\right)\left(\mathbf{S}_e \cdot \mathbf{v}_{\rm el}^{\perp}\right)$
$\mathcal{O}_5 = i\mathbf{S}_\chi \cdot \left(\frac{\mathbf{q}}{m_e} \times \mathbf{v}_{\rm el}^{\perp}\right)$	$\mathcal{O}_{10} = i\mathbf{S}_e \cdot \frac{\mathbf{q}}{m_e}$	$\mathcal{O}_{15} = i\mathcal{O}_{11}\left[\left(\mathbf{S}_e \times \mathbf{v}_{\rm el}^{\perp}\right) \cdot \frac{\mathbf{q}}{m_e}\right]$
$\mathcal{O}_6 = \left(\mathbf{S}_\chi \cdot \frac{\mathbf{q}}{m_e}\right)\left(\mathbf{S}_e \cdot \frac{\hat{\mathbf{q}}}{m_e}\right)$	$\mathcal{O}_{11} = i\mathbf{S}_\chi \cdot \frac{\mathbf{q}}{m_e}$	

Table 1: Interaction operators spanning the NR-EFT of spin 1/2 DM-electron interactions [2, 3, 4]. $\mathbf{S}_e$ ($\mathbf{S}_\chi$) denotes the electron (DM) spin, $\mathbf{v}_{\rm el}^{\perp} = \mathbf{v} - \boldsymbol{\ell}/m_e - \mathbf{q}/(2\mu_{\chi e})$, where $\mu_{\chi e}$ is the reduced mass of the DM-electron system and $\mathbb{1}_{\chi e}$ is the identity in the DM-electron spin space.

and $\widehat{\eta}$ is the velocity integral, q is the transferred momentum and ΔE is the deposited energy. $\mathbf{\Delta G}$ is a relative reciprocal lattice vector, and $\mathbf{k}$ ($\mathbf{k}'$) and i (i') denotes the initial (final) brillouin zone momentum and crystal band index, respectively. R_l is the DM response function and depends on DM physics, whereas $\overline{W}_l$ is the crystal response function and depends on crystal physics. $\overline{W}_l$ differ with the different B_l,

$$B_1 = \left|f'_{i,\mathbf{k}\to i',\mathbf{k}'}\right|^2 \qquad B_2 = \frac{\mathbf{q}}{m_e} \cdot (f'_{i,\mathbf{k}\to i',\mathbf{k}'})(\mathbf{f}'_{i,\mathbf{k}\to i',\mathbf{k}'})^*$$
$$B_3 = \left|\mathbf{f}'_{i,\mathbf{k}\to i',\mathbf{k}'}\right|^2 \qquad B_4 = \left|\frac{\mathbf{q}}{m_e} \cdot \mathbf{f}'_{i,\mathbf{k}\to i',\mathbf{k}'}\right|^2$$
$$B_5 = i\frac{\mathbf{q}}{m_e} \cdot \left[\mathbf{f}'_{i,\mathbf{k}\to i',\mathbf{k}'} \times \left(\mathbf{f}'_{i,\mathbf{k}\to i',\mathbf{k}'}\right)^*\right] \tag{4}$$

where

$$f'_{i,\mathbf{k}\to i',\mathbf{k}'} \equiv \sum_{\mathbf{G}} u_{i'}^*\left(\mathbf{k}' + \mathbf{G} + \mathbf{\Delta G}\right) u_i\left(\mathbf{k} + \mathbf{G}\right) \tag{5}$$

$$\mathbf{f}'_{i,\mathbf{k}\to i',\mathbf{k}'} \equiv -\frac{1}{m_e}\sum_{\mathbf{G}} u_{i'}^*\left(\mathbf{k}' + \mathbf{G} + \mathbf{\Delta G}\right)\left(\mathbf{k} + \mathbf{G}\right) u_i\left(\mathbf{k} + \mathbf{G}\right)\,, \tag{6}$$

and the coefficients $u_i(\mathbf{k} + \mathbf{G})$ come from the Bloch wave-function,

$$\psi_{i\mathbf{k}}(\mathbf{x}) = \frac{1}{\sqrt{V}}\sum_{\mathbf{G}} u_i(\mathbf{k} + \mathbf{G}) e^{i(\mathbf{k}+\mathbf{G})\cdot\mathbf{x}}\,. \tag{7}$$

For the dark photon model, the only non-zero DM response is R_1, and therefore $\overline{W}_1$ was the only previously known crystal response functions. The other 4 are novel and identified in [1] for the first time.

3. Results

$\overline{W}_l$ is evaluated by `QEdark-EFT` [5], an extension to the `QEdark` package [6], interfacing with the DFT code `QuantumEspresso v.5.1.2` [7]. The rate is evaluated with $v_0 = 220$ km sec^{-1} [8] being the most probable velocity in the galactic rest frame, $v_{\rm esc} = 544$ km sec^{-1} [9] being the local escape velocity, $v_\oplus = 244$ km sec^{-1} being the earth velocity in the galactic rest frame and $n_\chi = 0.4$ GeV/cm$^3/m_\chi$ [10] being the local DM density. To illustrate what can be done with our framework we take the examples of the anapole and magneitc dipole interactions, whose Lagrangians are given as

$$\mathscr{L}_{\rm anapole} = \frac{g}{2\Lambda^2}\,\overline{\chi}\gamma^\mu\gamma^5\chi\,\partial^\nu F_{\mu\nu}\,, \qquad \mathscr{L}_{\rm magnetic} = \frac{g}{\Lambda}\,\overline{\psi}\sigma^{\mu\nu}\psi\,F_{\mu\nu}\,, \tag{8}$$

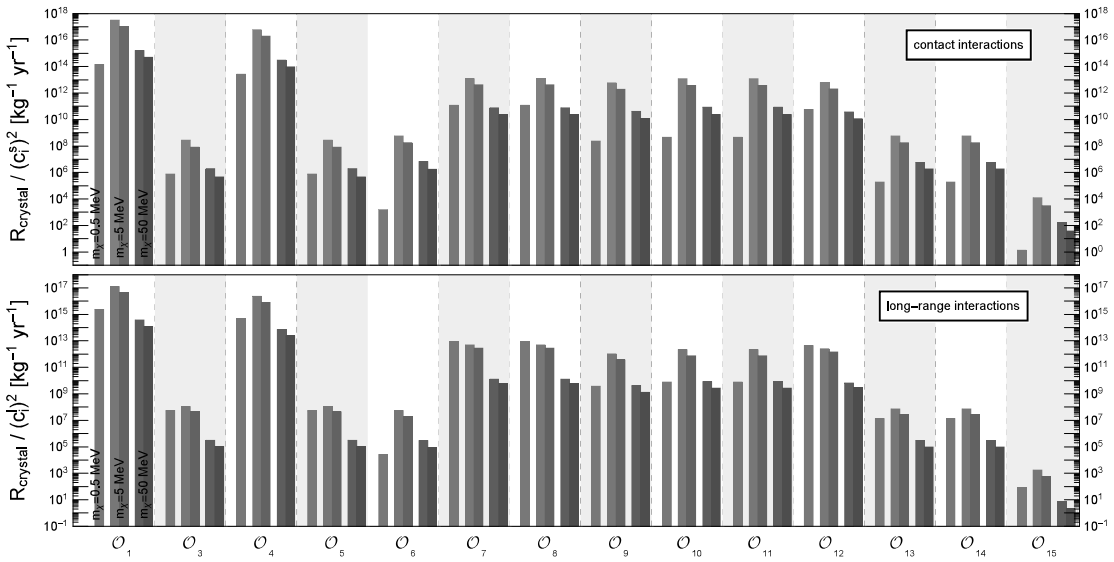

Figure 1: Rate contributions from operators $\mathcal{O}_1$ to $\mathcal{O}_{15}$ from table 1 for silicon (blue) and germanium (red), with DM masses of 0.5 MeV (left), 5 MeV (middle) and 50 MeV (right). For $m_\chi = 0.5\,\text{MeV}$ the expected excitation rate in silicon is 0 due to the larger band gap.

where $F_{\mu\nu} = \partial_\mu A_\nu - \partial_\nu A_\mu$ is the photon field strength tensor, and A^ν the photon field. In the non-relativistic limit, the free electron scattering amplitudes associated with the above Lagrangians are [4]

$$\mathscr{M}_{\text{anapole}} = \frac{4eg}{\Lambda^2} m_\chi m_e \left\{ 2\left(\mathbf{v}_{\text{el}}^\perp \cdot \xi^{\dagger s'} \mathbf{S}_\chi \xi^s\right) \delta^{\lambda'\lambda} + g_e \left(\xi^{\dagger s'} \mathbf{S}_\chi \xi^s\right) \cdot \left(i\frac{\mathbf{q}}{m_e} \times \xi^{\dagger \lambda'} \mathbf{S}_e \xi^\lambda\right) \right\} \tag{9}$$

$$\begin{aligned}\mathscr{M}_{\text{magnetic}} = \frac{eg}{\Lambda} \Bigg\{ & 4m_e \delta^{s's} \delta^{\lambda'\lambda} + \frac{16 m_\chi m_e}{q^2} i\mathbf{q} \cdot \left(\mathbf{v}_{\text{el}}^\perp \times \xi^{\dagger s'} \mathbf{S}_\chi \xi^s\right) \delta^{\lambda'\lambda} \\ & - \frac{8 g_e m_\chi}{q^2} \left[\left(\mathbf{q} \cdot \xi^{\dagger s'} \mathbf{S}_\chi \xi^s\right) \left(\mathbf{q} \cdot \xi^{\dagger \lambda'} \mathbf{S}_e \xi^\lambda\right) - q^2 \left(\xi^{\dagger s'} \mathbf{S}_\chi \xi^s\right) \cdot \left(\xi^{\dagger \lambda'} \mathbf{S}_e \xi^\lambda\right) \right] \Bigg\}, \end{aligned} \tag{10}$$

where $g_e \simeq 2$ is the electron g-factor. From the free electron scattering amplitudes above we find that

$$c_8^s = 8 e m_e m_\chi \frac{g}{\Lambda^2}\,, \qquad\qquad c_9^s = -8 e m_e m_\chi \frac{g}{\Lambda^2}\,, \tag{11}$$

are the only non-zero coupling constants for the anapole interaction and

$$\begin{aligned} c_1^s &= 4 e m_e \frac{g}{\Lambda}\,, & c_4^s &= 16 e m_\chi \frac{g}{\Lambda}\,, \\ c_5^\ell &= \frac{16 e m_e^2 m_\chi}{q_{\text{ref}}^2} \frac{g}{\Lambda}\,, & c_6^\ell &= -\frac{16 e m_e^2 m_\chi}{q_{\text{ref}}^2} \frac{g}{\Lambda}\,. \end{aligned} \tag{12}$$

are the non-zero ones for the magnetic dipole interaction. In fig. 2 the rate spectrum and exclusion limits for these models are presented for the anapole interaction to the left and the magnetic dipole interaction to the right. The dash-dotted lines in the 4 uppermost panels show

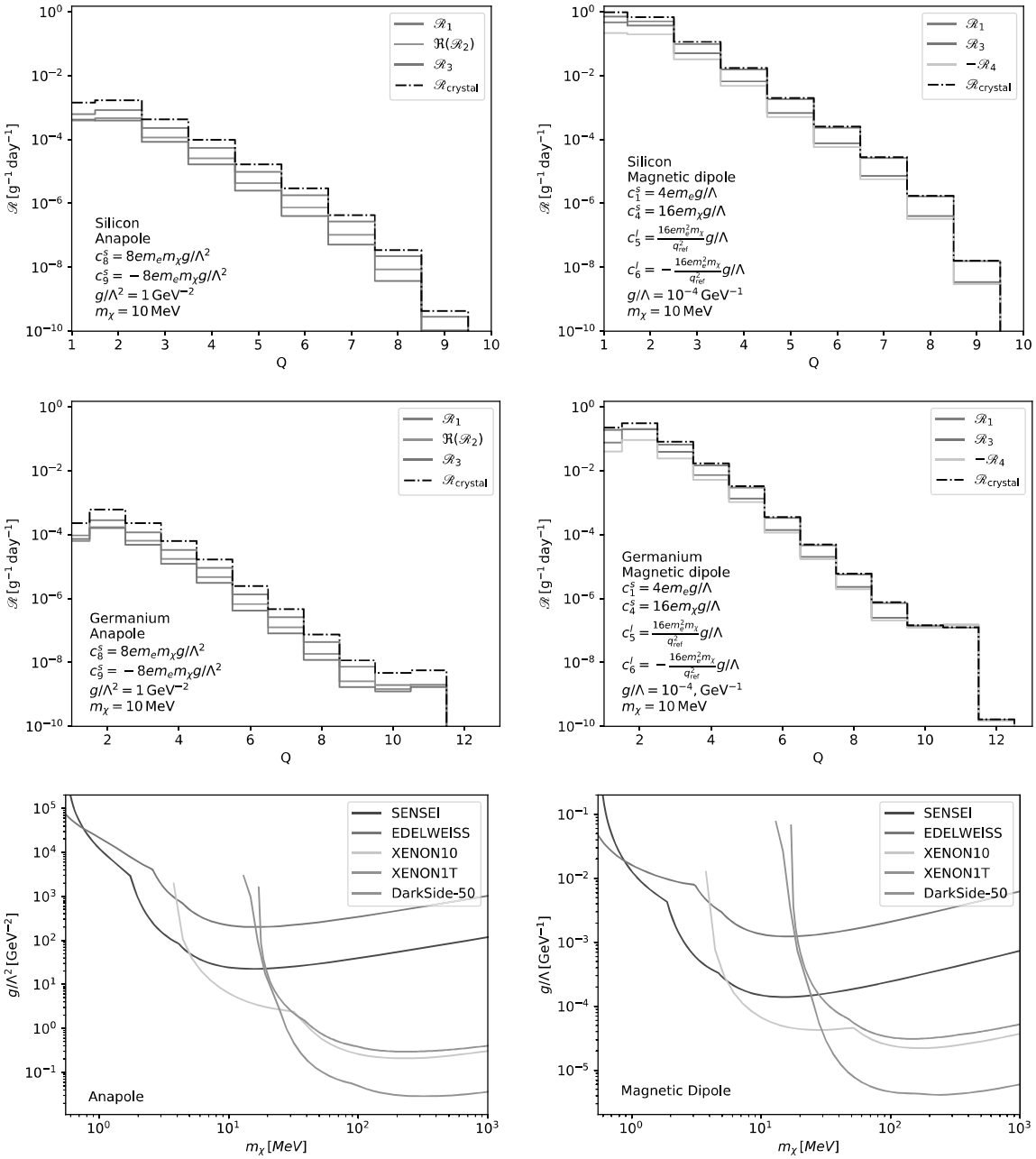

Figure 2: Expected rates of events creating Q electron hole pairs in silicon (top), germanium (middle) and 90% C.L. limits (bottom) for anapole (magnetic dipole) interaction to the left (right). In the rate plots the black dash-dotted line denotes the total rate, whereas the colored lines show the contributions of the individual DM crystal response products. The nobel gas limits are from [4], whereas the SENSEI@MINOS [11] and EDELWEISS [12] limits are from [1].

the rate of events creating Q electron hole pairs, and the colored lines show the contributions of individual DM crystal response products $\mathscr{R}_l$, $\mathscr{R}_{\text{crystal}} = \sum_{l=1}^{5} \mathscr{R}_l$. Note that for the magnetic dipole case $\mathscr{R}_4$ gives a negative contribution to the event rate. In the lower two panels we show the exclusion limits current experiments set on these models. Note that germanium gives the strongest constraint below an MeV due to it having a smaller band gap than silicon, allowing it to probe lower deposited energies. The anapole and magnetic dipole interactions could not be modelled previously, and serve to illustrate the power of our general framework.

References

[1] Riccardo Catena et al. "Crystal responses to general dark matter-electron interactions". In: *Phys. Rev. Res.* 3.3 (2021), p. 033149. DOI: 10.1103/PhysRevResearch.3.033149. arXiv: 2105.02233 [hep-ph].

[2] JiJi Fan, Matthew Reece, and Lian-Tao Wang. "Non-relativistic effective theory of dark matter direct detection". In: *JCAP* 1011 (2010), p. 042. DOI: 10.1088/1475-7516/2010/11/042. arXiv: 1008.1591 [hep-ph].

[3] A. Liam Fitzpatrick et al. "The Effective Field Theory of Dark Matter Direct Detection". In: *JCAP* 1302 (2013), p. 004. DOI: 10.1088/1475-7516/2013/02/004. arXiv: 1203.3542 [hep-ph].

[4] Riccardo Catena et al. "Atomic responses to general dark matter-electron interactions". In: *Phys. Rev. Res.* 2.3 (2020), p. 033195. DOI: 10.1103/PhysRevResearch.2.033195. arXiv: 1912.08204 [hep-ph].

[5] Einar Urdshals and Marek Matas. *QEdark-EFT*. Version 0.1.0. May 2021. DOI: 10.5281/zenodo.4739187. URL: https://doi.org/10.5281/zenodo.4739187.

[6] Rouven Essig et al. "Direct Detection of sub-GeV Dark Matter with Semiconductor Targets". In: *JHEP* 05 (2016), p. 046. DOI: 10.1007/JHEP05(2016)046. arXiv: 1509.01598 [hep-ph].

[7] P Giannozzi et al. "Advanced capabilities for materials modelling with Quantum ESPRESSO". In: *Journal of Physics: Condensed Matter* 29.46 (Oct. 2017), p. 465901. DOI: 10.1088/1361-648x/aa8f79. URL: https://doi.org/10.1088/1361-648x/aa8f79.

[8] F. J. Kerr and Donald Lynden-Bell. "Review of galactic constants". In: *Mon. Not. Roy. Astron. Soc.* 221 (1986), p. 1023.

[9] Martin C. Smith et al. "The RAVE Survey: Constraining the Local Galactic Escape Speed". In: *Mon. Not. Roy. Astron. Soc.* 379 (2007), pp. 755–772. DOI: 10.1111/j.1365-2966.2007.11964.x. arXiv: astro-ph/0611671.

[10] Riccardo Catena and Piero Ullio. "A novel determination of the local dark matter density". In: *JCAP* 08 (2010), p. 004. DOI: 10.1088/1475-7516/2010/08/004. arXiv: 0907.0018 [astro-ph.CO].

[11] Liron Barak et al. "SENSEI: Direct-Detection Results on sub-GeV Dark Matter from a New Skipper-CCD". In: *Phys. Rev. Lett.* 125.17 (2020), p. 171802. DOI: 10.1103/PhysRevLett.125.171802. arXiv: 2004.11378 [astro-ph.CO].

[12] Q. Arnaud et al. "First germanium-based constraints on sub-MeV Dark Matter with the EDELWEISS experiment". In: *Phys. Rev. Lett.* 125.14 (2020), p. 141301. DOI: 10.1103/PhysRevLett.125.141301. arXiv: 2003.01046 [astro-ph.GA].